International Journal of Science and Research Archive

eISSN: 2582-8185

Cross Ref DOI: 10.30574/ijsra

Journal homepage: https://ijsra.net/

(RESEARCH ARTICLE)

Check for updates

Identification of alteration zones using remote sensing lineaments; Optic and radar images in the case of the departments of Abtouyour and Guéra (central massif of Chad)

AMINE KARIFENE [1], PODO MAHAMAT MATAR [2, *], MACKAYE HASSAN TAISSO [2], MAMADOU MALLOUM AHMAT [1], MAHAMAT ALI ATEIB [1] and CHRISTIAN NGOMA MVOUNDOU [3]

[1] *Department of Geomatics, Faculty of Mines and Geology, Polytechnic University of Mongo (Chad).*
[2] *Department of Geosciences, Faculty of Exact and Applied Sciences, University of Ndjamena (Chad).*
[3] *Laboratory of Mechanics Energy and Engineering, Higher National Polytechnic School, Marien NGOUABI University (CONGO).*

International Journal of Science and Research Archive, 2024, 12(02), 1890–1901

Publication history: Received on 29 June 2024; revised on 06 August 2024; accepted on 09 August 2024

Article DOI: https://doi.org/10.30574/ijsra.2024.12.2.1457

Abstract

This work concerns the extraction of lineaments likely to control mineralization from OLI 2 (Landsat 9) and Palsar satellite images. The lineaments were first extracted from OLI2 images. Principal component analyses, directional filters (ENVI 5.3 software) and the Line tool (Geomatica PCI) were used to generate the lineaments. Structural information was then extracted using Palsar radar images. Directional filters and the Line tool were used to produce the lineaments of the area. Directional rosettes were produced using Rockwork software. One thousand five hundred and five (1505) lineaments extracted from Palsar images, the longest of which has a length of 10,514 m with a total length of lineaments of 371,938.05 while eight hundred and thirty-five (835) lineaments are extracted from Landsat images, with a maximum lineament length of 20,970 m and a total length of 583,615.26 m. The major directions of the lineaments are **N150, N00, N30** and **N165**. These major directions coincide with the major directions of the old works in the study area. The validation of the results obtained was carried out using geophysical data from the area and these data confirm the effectiveness of the results.

Keywords: Lineaments; Satellite images; Guéra; Geophysical data

1. Introduction

Knowledge of geology is of great importance in identifying mineral substances in a country. Structural information is even more decisive in the concentration of valuable substances. Important studies are carried out to identify faults, fractures to characterize structures that control mineralization [1], [2], [3] on the one hand, and structures that control the constitution of basement aquifers on the other hand [4], (Mohammad pour et al., 2020), [6], [7], [8], [9], [10], [11]. To make the structural study more efficient, several authors have used satellite image technology and GIS to extract structural information [12], [13], [12], [14], [15], [16]. Classical structural studies do not allow the exhaustive identification of lineaments, the implementation time of the classical approach is very long and to obtain good results, this approach is very tedious and expensive. To meet these challenges, many studies have focused on the use of this new technology and very good results have been obtained worldwide. To experiment with this approach, optical and radar satellite images are used to extract the lineaments of the Abtouyour and Guéra departments, central massif of Chad. The objective of this work is to extract the lineaments of the study area.

* Corresponding author: S PODO MAHAMAT MATAR

1.1. Location of the study area

The study area is located between 17°30' and 19° east longitude, and 11° and 13° north latitude. The study area includes two departments: the department of Guéra and the department of Abtouyour. These two departments belong to the province of Guéra; the city of Mongo is the capital of the province, Figure 1 shows the location of the study area.

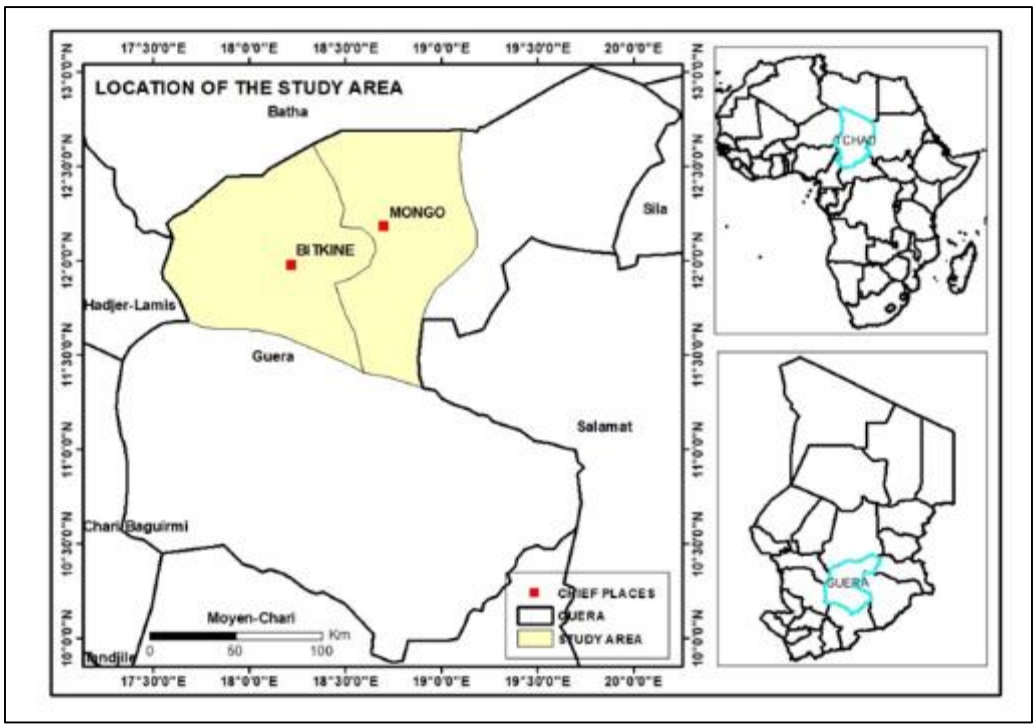

Figure 1 Location of the study area

1.2. Regional geological framework

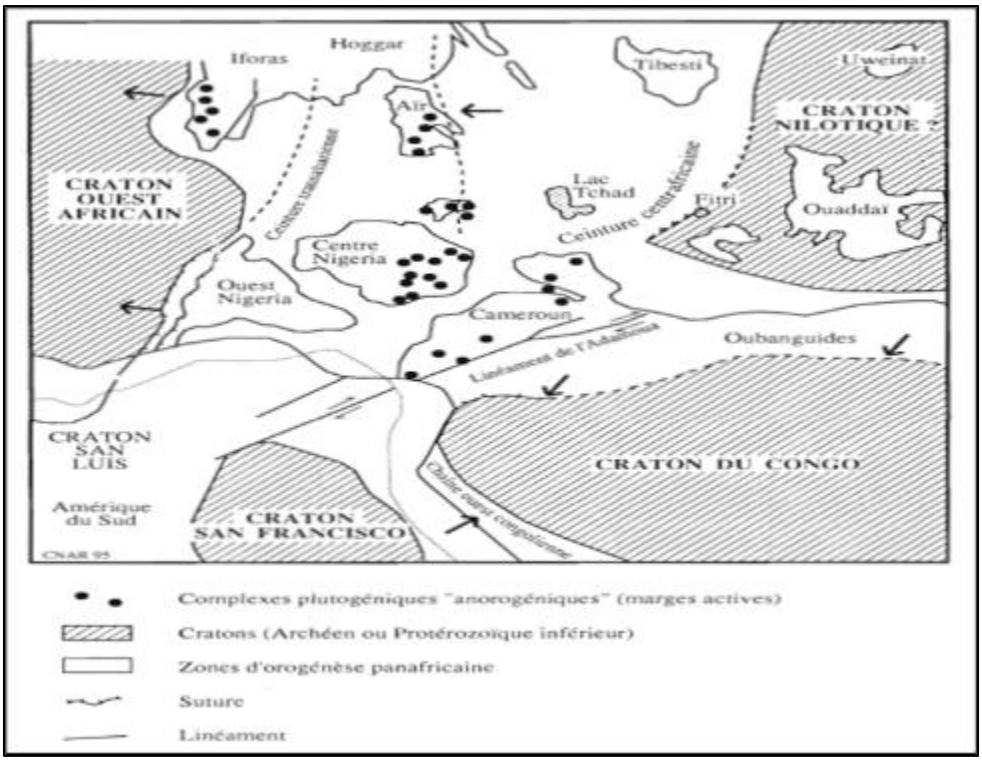

Figure 2 Location of cratonic and mobile zones in Central Africa

Geologically, Chad belongs to the Pan-African mobile zone, limited to the south by the Congo craton, to the west by the West African craton and to the northeast by the Nilotic craton [17] and includes the Uweinat craton. The northern boundary with the Nilotic craton is very poorly defined and its southern boundary with the Congo craton is materialized by the Sanaga shear zone in Cameroon. However, the concept of Nilotic craton and Uweinat has been questioned, because the geological formations of these cratons have different ages proving that some formations were remobilized by the Pan-African orogeny. [18] Proposed the concept of metacraton whose arguments put forward convinced the scientific community and helped to remove concerns about the ages of the formations. Therefore, the Tibesti, Ouaddaï and Massif Central formations belong to the Sahara metacraton while the Mayo Kebbi and Baibokoum massifs belong to the Central African mobile zone. The Pan-African orogeny is at the origin of the formation of sedimentary basins (Doba basin, Lake Chad basin, Ennedi basin and the Tibesti basin) made up of recent sedimentary formations [19].

1.3. Geological framework of the Guéra province

The Guéra province is part of the Sahara metacraton constituting the central Chadian massif, formed mainly by the Guéra and Aboutelfan massifs and some smaller outcrops. These massifs result from the collision between the Congo craton and the Saharan metacraton [18] [20] [19] [21]. The Guéra massif constitutes one of the smallest massifs of the Sahara metacraton, comprising magmatic and metamorphic rocks dating from the Neoproterozoic covered by quaternary sediments. The granitoids of the province are grouped into two: those, which are old, metalluminous to peralluminous, magnesian and alkaline, collisional, and those, which are young, peralluminous, ferrous, calco-alkaline, and post-collisional. Overall, the province is petro graphically composed of granites, granodiorites, diorites and gneisses with basaltic enclaves and cut by pegmatitic, aplitic veins and dolerite dykes. Between these formations are recent sedimentary covers.

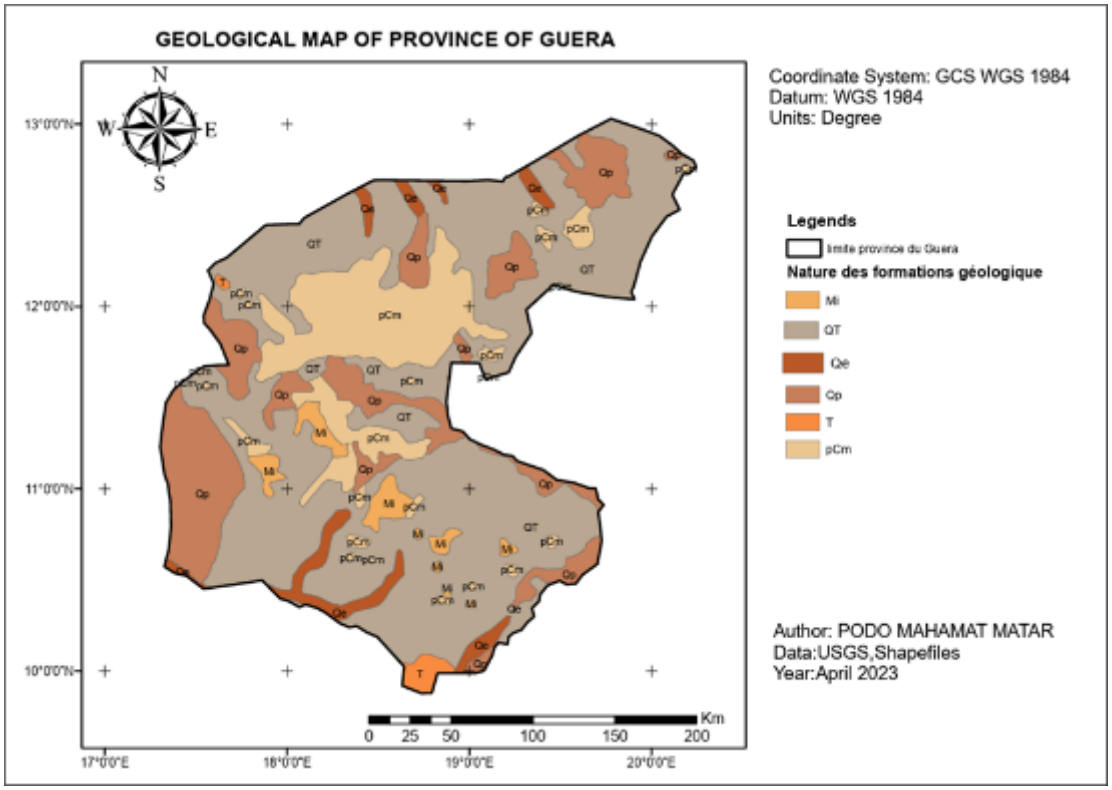

Figure 3 Geological map of the Guéra province

2. Materials and Method

2.1. Materials and Data

Image data composed of OLI and Palsar images were used to extract the lineaments of the study area. The Landsat 9 satellite has two sensors: the Operation Land Imager (OLI) sensor and the Thermal Infrared (TIR) sensor, which provide images in eleven (11) bands. The characteristics of the data from these sensors are shown in Table 1. Scenes 182052 and 182051 are used to cover the study area.

Table 1 Characteristics of Landsat 9 images

Band	Spatial Resolution (m)	Spectral Resolution (µm)
Band 1(Aerosol/Costal)	30	0.435 – 0.451
Band 2 (Blue)	30	0.452 – 0.512
Band 3 (Green)	30	0.533 – 0.590
Band 4 (Red)	30	0.636 – 0.673
Band 5 (Near Infrared)	30	0.851 – 0.879
Band 6 (Mid Infrared 1)	30	1.566 – 1.651
Band 7 (Mid Infrared 2)	30	2.107 – 2.294
Band 8 (Panchromatic)	15	0.503 – 0.676
Band 9 (Cirus)	30	1.363 – 1.384
Band 10 (Thermal Infrared 1)	100	10.60 – 11.19
Band 11 (Thermal Infrared 2)	100	11.50 – 12.51

PALSAR images from the Japanese ALOS PALSAR satellite in dual polarization mode (HH and HV) and Fine Resolution Mode are also used. Twelve mosaicked PALSAR scenes covering the study area are integrated in this study for lineament extraction. The pixel size is 14.384536m x 15.28764m. The characteristics of these data are summarized in Table 2.

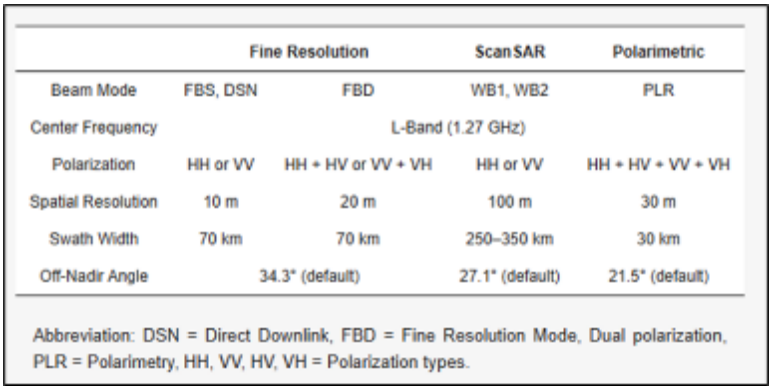

	Fine Resolution		ScanSAR	Polarimetric
Beam Mode	FBS, DSN	FBD	WB1, WB2	PLR
Center Frequency	L-Band (1.27 GHz)			
Polarization	HH or VV	HH + HV or VV + VH	HH or VV	HH + HV + VV + VH
Spatial Resolution	10 m	20 m	100 m	30 m
Swath Width	70 km	70 km	250–350 km	30 km
Off-Nadir Angle	34.3° (default)		27.1° (default)	21.5° (default)

Abbreviation: DSN = Direct Downlink, FBD = Fine Resolution Mode, Dual polarization, PLR = Polarimetry, HH, VV, HV, VH = Polarization types.

Figure 4 Characteristics of ALOS PALSAR data

Vector data with the administrative boundaries of Chad were used to produce the study location map. They also allowed the extraction of the study area in order to extract the Landsat 8 and Palsar mosaic scenes.

Software was used for data processing

- Arc Gis 10.8 software to produce the lineament map and the location map;
- Envi 5.3 software for processing optical (Landsat 8) and Radar (Palsar) satellite images;
- PCI Geomatica software for automatic lineament extraction;
- Rockwork software for determining the major directions of the lineaments.
- A Lenovo Thinpack T460S brand computer, core i7 12G of Ram 500G of SSD hard drive serving as a platform for the software;
- A GPS for extracting coordinates.

2.2. Method

2.2.1. Landsat image processing method

Pre-processing of Landsat 9 images

The radiometric and atmospheric corrections performed on Landsat 8 images constitute the bulk of the pre-processing operations. The radiometric calibration is performed because of the errors that are due to the irregularities of the

sensors. The radiometric calibration module of the Envi 5.3 software performs it while the atmospheric correction is done to eliminate the atmospheric disturbances caused by the constituent elements of the atmosphere. The Flash atmospheric correction module of the Envi 5.3 software is used to perform the atmospheric correction. Many authors have obtained good results by performing radiometric and atmospheric corrections to reduce the noise included in the images [1], [15], [22], [23], [4]. After the corrections, the two Landsat scenes were mosaicked in order to extract the study area.

Landsat 9 image processing

Data processing for lineament extraction involves several phases: fusion of panchromatic and multispectral data, calculation of Principal Component Analysis (PCA), directional filtering in the four (4) directions (N45, N90, N135 and N180) and automatic lineament extraction.

The fusion of panchromatic and multispectral data allowed, on the one hand, the improvement of the spatial resolution of the multispectral bands (30m to 15m) and on the other hand the improvement of the spectral resolution of the panchromatic band. The resulting images have a good spectral resolution and a spatial resolution of 15m. PCA is applied to obtain a new dataset with better essential information from the original dataset [24]. A PCA was generated using the seven bands of the resulting images producing three main components PC1, PC2 and PC3. A RGB coloured composition (PC1 PC2 PC3) was made.

The fusion of the images, the PCAs, the coloured composition and the directional filters were made using the ENVI 5.3 software. Directional filters (N45, N90, N135 and N180) are made on the obtained image (PCA coloured composition). The automatic extraction of lineaments was possible thanks to the Line module of Geomatica, which is based on six parameters:

- RADI, (filter radius in pixels).

The radius of the Gaussian filter that will be used in the detection of edges;

- GTHR (Edge Gradient Threshold) constitutes the value of the gradient to be taken as an edge detection threshold for the binarisation of the image:
- LTHR (Curve Length Threshold) (in pixels), the minimum length of a curve to be taken as a lineament;
- FTHR (Line Fitting Threshold) (in pixels): The tolerance allowed in the adjustment of the curve (results of the previous parameter) to form a polyline;
- ATHR (Angular Difference Threshold) (in degrees): Defines the angle not to be exceeded between two polylines to be connected.
- DTHR (Linking Distance Threshold) (in pixels): The maximum distance between two polylines to be connected.

Several works have successfully tested these six parameters allowing automatic extraction: [22], [14], [15], [25], [24]. The values of these six parameters are calibrated and adapted to obtain a better adjustment and allow efficient extraction of lineaments. The values allowing the extraction of lineaments are presented in Table 2.

Table 2 The six parameters for PCI software lineament extraction Table 2: The six parameters for PCI software lineament extraction

Parameters	**Values**
RADI, (rayon du filtre en pixel)	20
GTHR (Edge Gradient Threshold)	150
LTHR (Curve Length Threshold) (en pixels)	180
FTHR (Line Fitting Threshold) (en pixels)	10
ATHR (Angular Difference Threshold)	15
DTHR (Linking Distance Threshold)	150

The extracted lineaments are saved in Shape format and exported to Arc GI 10.8 software for refinement, validation and layout.

2.2.2. Palsar image processing method

Palsar images are processed by ENVI 5.3 software; these images are corrected for salt and pepper effects, irregularities in radar images. This correction is performed using Frost and Lee filters, which allowed the images to be cleaned of these salts and pepper effects. Four (4) directional filters are generated from the corrected images: the N-S filter, the NE-SW filter, the NW-SE filter and the E-W filter. The four resulting filters were automatically extracted from the lineaments and the latter are exported and processed using ArcGIS 10.8 software. The validation of these lineaments is done using geophysical data, field data, images and the road network.

3. Results analysis and interpretation

3.1. Principal component analysis of the study area

Figure 2 presents the principal component analysis generated with the seven Landsat 9 bands and three principal components generated, were subject to RGB coloured composition, ACP1 ACP2 ACP3.

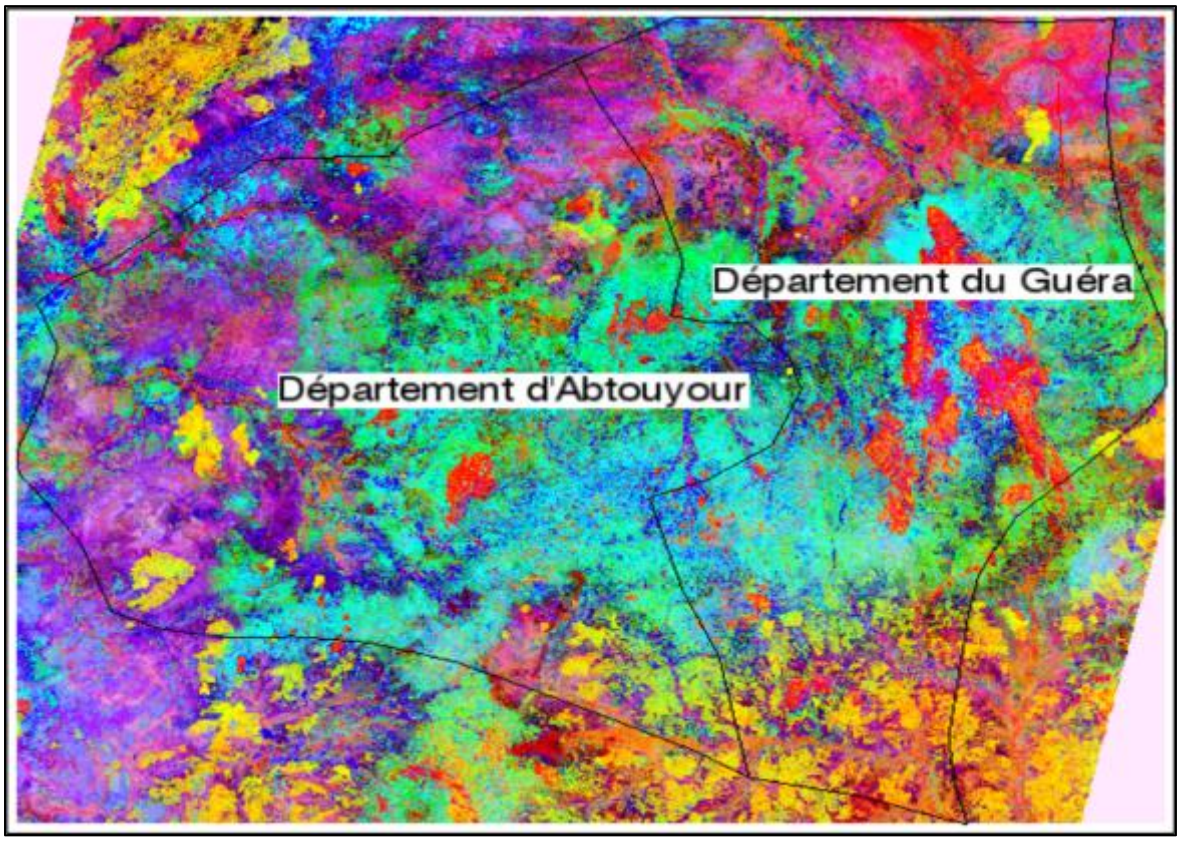

Figure: 5 Colour composition of the principal component analysis (ACP1 ACP2 ACP3)

Figure 5 shows the four directional filters produced from the image resulting from the coloured composition of the ACP principal components.

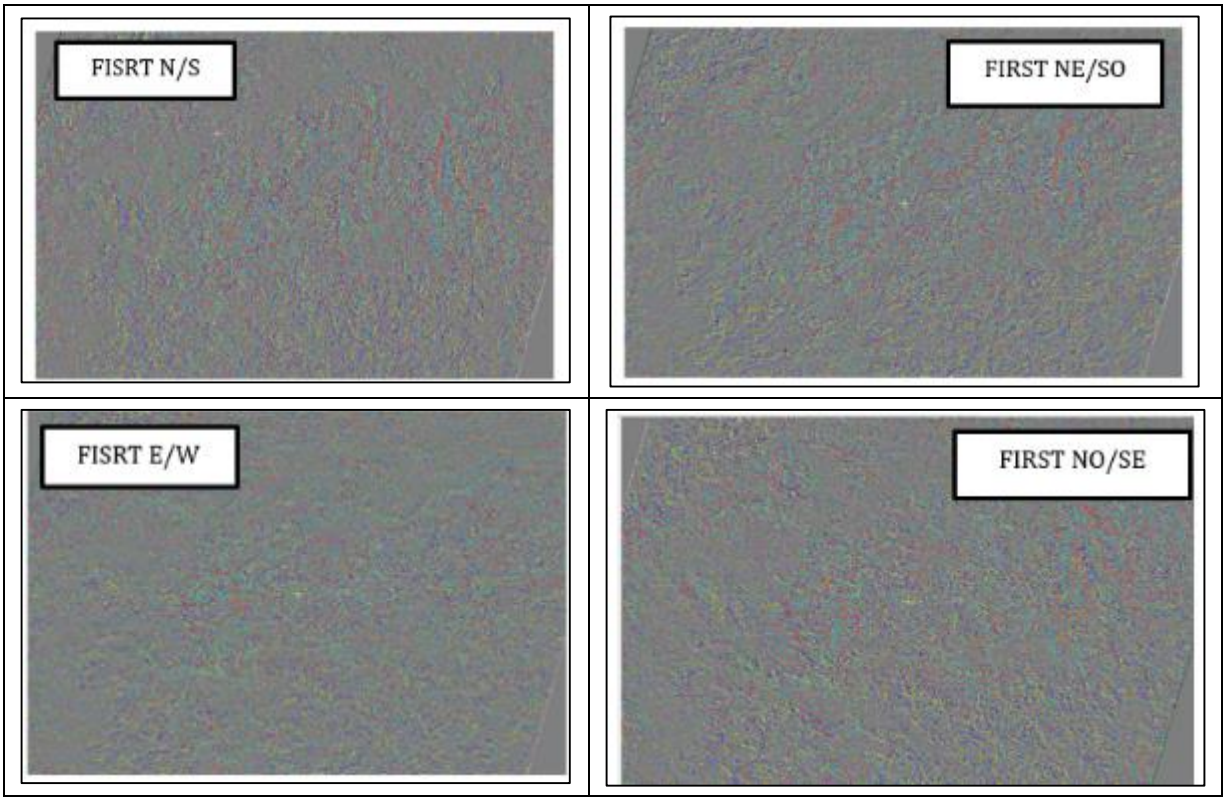

Figure: 6 NS, NESO, NOSE and EO directional filters generated from Landsat 9 images

3.2. Presentation of lineaments extracted from Landsat 9 data.

Figure 7 presents the map of lineaments extracted from Landsat 9 images.

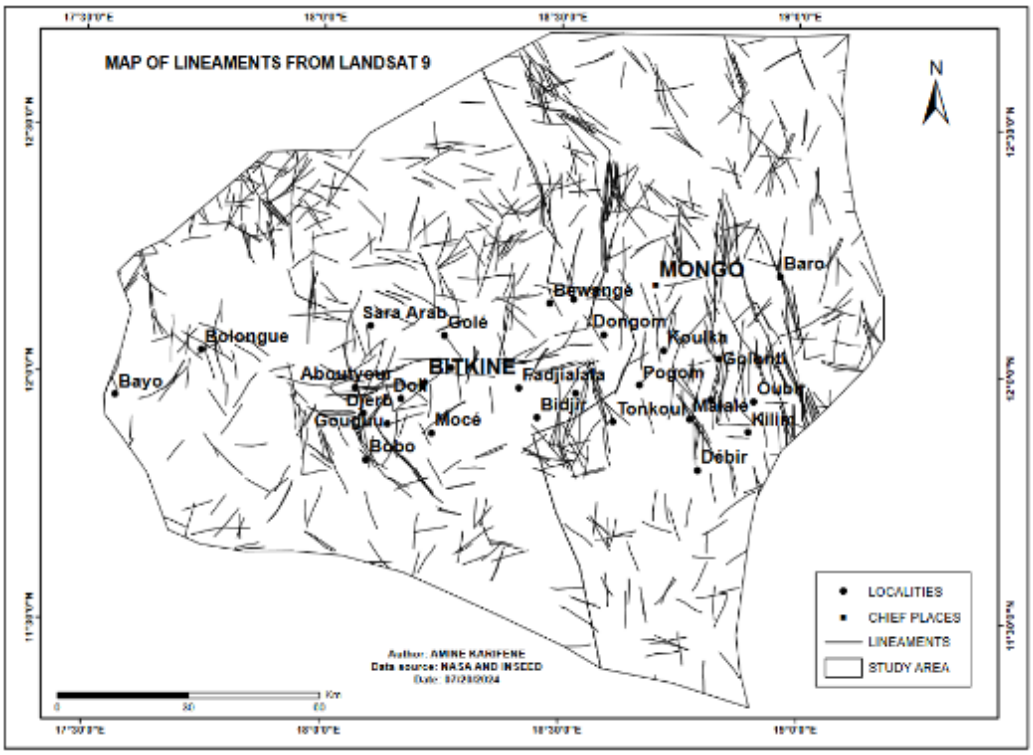

Figure: 7 Lineament map from Landsat 9 images

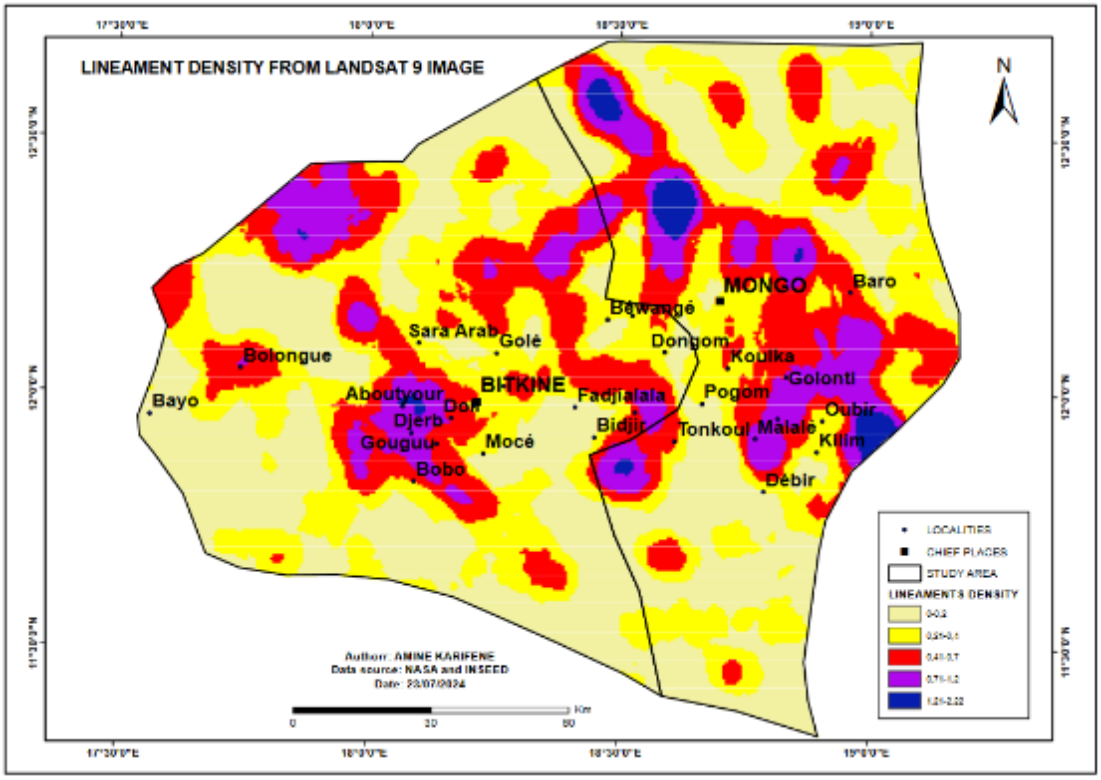

Figure 8 Density map of lineaments from Landsat 9 images

3.3. Presentation of lineaments extracted from Palsar images

The lineaments extracted from Palsar images are presented in Figure 8.

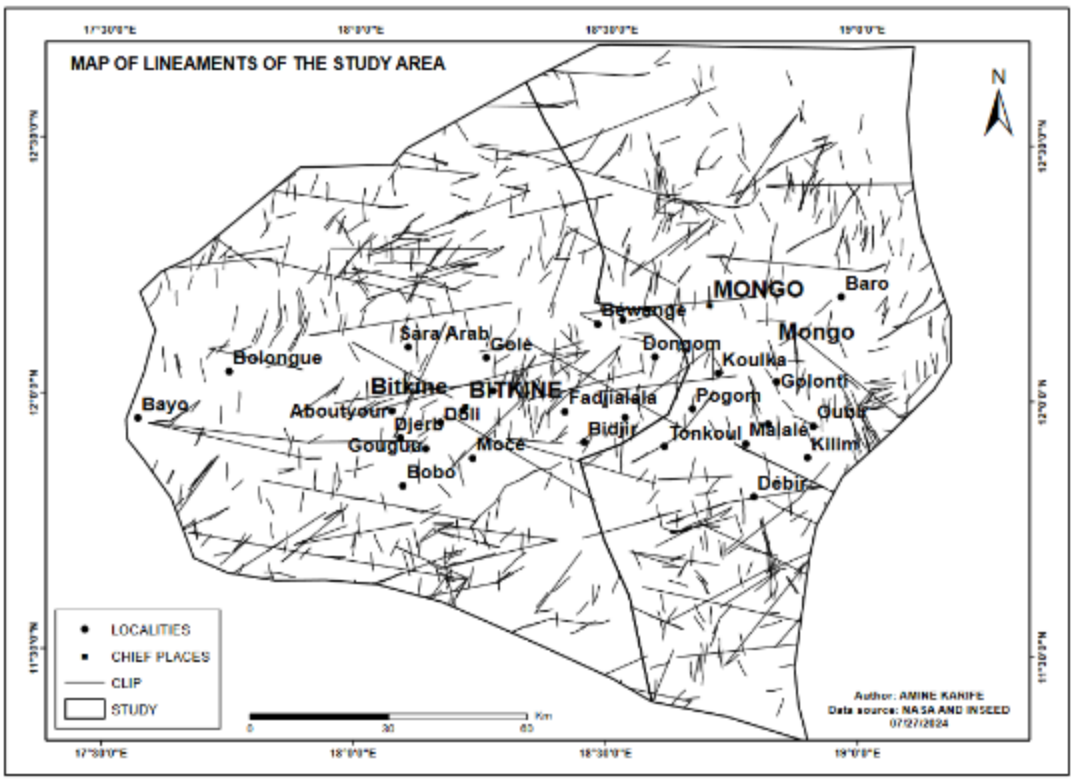

Figure 9 Lineament map from Palsar images

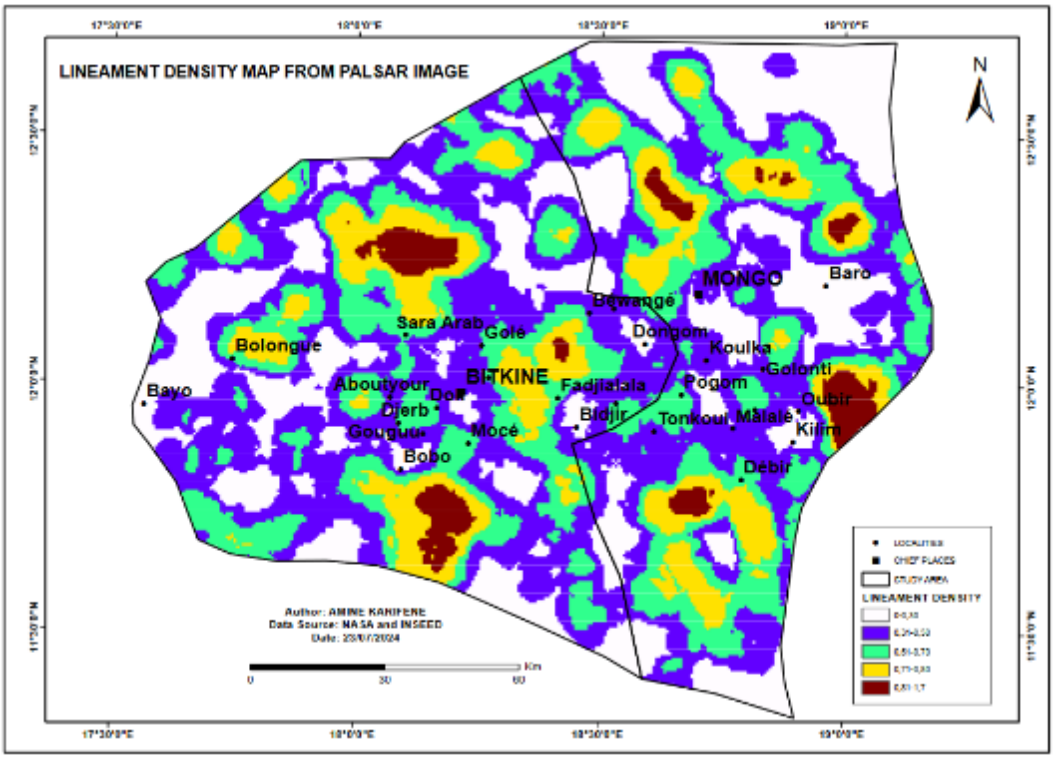

Figure 10 Lineament density map from Palsar images

3.4. Analysis and interpretation

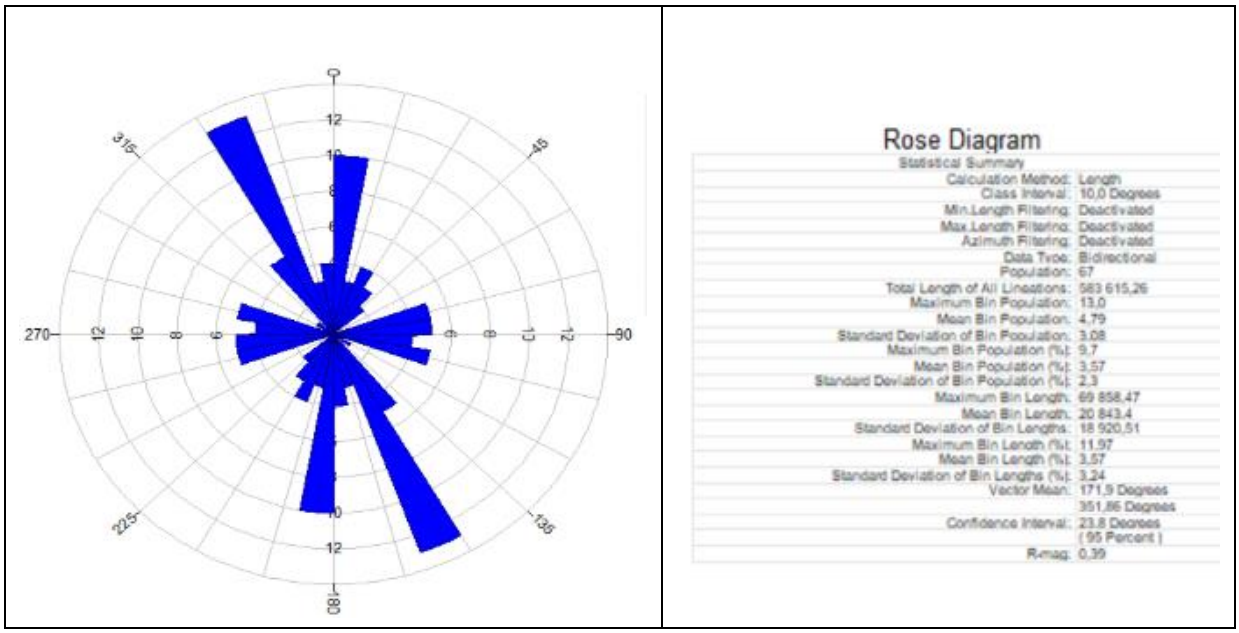

Figure 11 Directional rosette of lineaments from Landsat images

The lineaments extracted from Palsar radar images have a greater number of lineaments than those extracted from Landsat images. One thousand five hundred and five (1505) lineaments extracted from Palsar images, the longest of which has a length of 10,514 m with a total lineament length of 371,938.05 (Figure 12) while eight hundred and thirty-five (835) lineaments are extracted from Landsat images, with a maximum lineament length of 20,970 m and a total length of 583,615.26 m (Figure 11). The major directions of the lineaments are N150, N00, N30 and N165.

This analysis shows that the Palsar images are those, which allow the maximum extraction of lineaments, but the total length and the maximum length of these lineaments remain low compared to the Landsat 9 images.

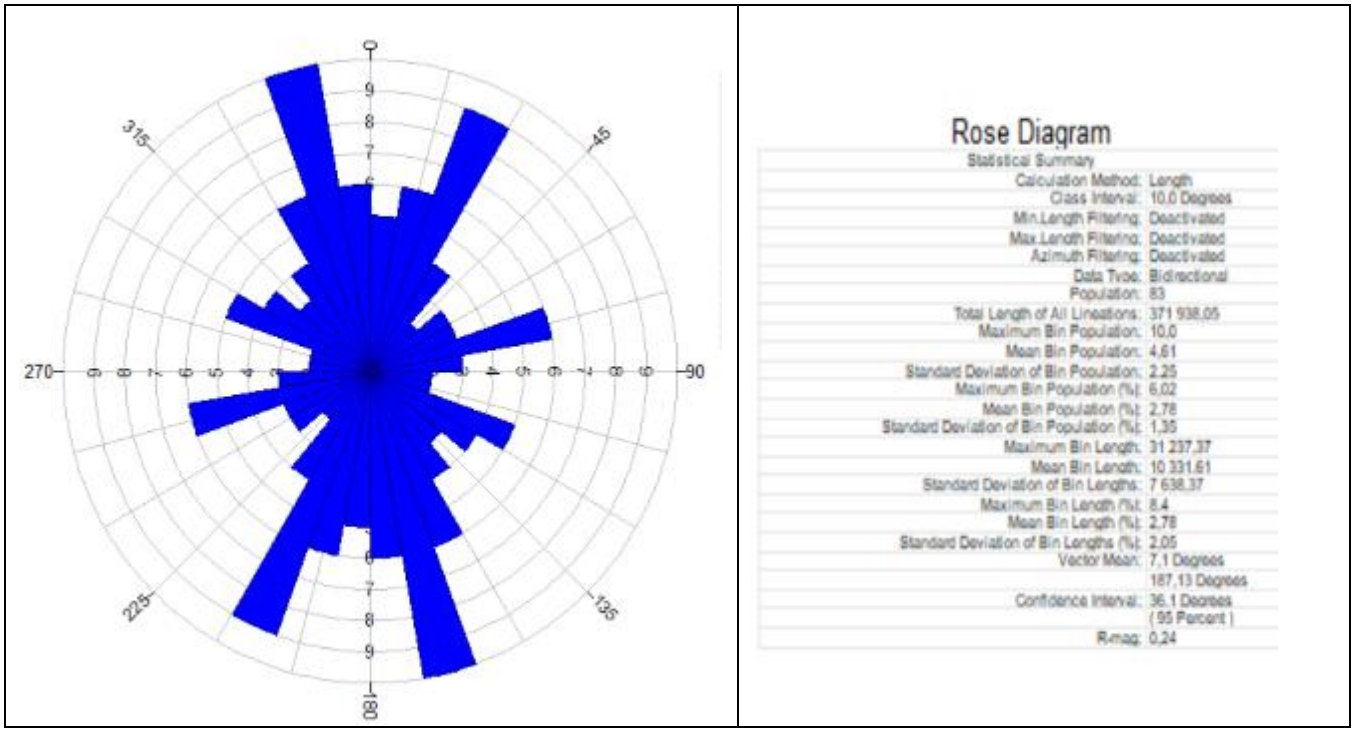

Figure: 12 Directional rosette of lineaments from Palsar images

It emerges from this analysis that radar images enhance linear structures better, this statement fits well with the work of [26], [16], [14], [15]…¬ this is the reason why the lineaments extracted via Palsar images were used for validation and the observation is satisfactory because the geophysical data for the location of drilling in the area show us that the positive drillings are positioned either on a fracture or on a fracture intersection.

4. Conclusion

The lineaments produced by the Palsar images have a number of 1505, the longest lineament has a length of 10514m and the total length of extracted lineaments is 371,938.05m. While the number of lineaments produced from Landsat 9 images is 835. The longest lineament is 20,970 m and the total length of the lineaments is 583,615.26 m. The major directions of the lineaments are N150, N00, N30 and N165. These directions are in line with previous work.

Compliance with ethical standards

Acknowledgments

Our thanks to the University of Mongo, which allowed us to carry out this work thanks to its laboratory and its President Professor MACKAYE HASS TAÏSSO for his guidance and availability and to the CDIG (Center for Documentation and Geographic Information) for the data, it provided us and the documentation.

Disclosure of conflict of interest

We affirm on our honour that all the authors who contributed to the writing of this article have no conflict of interest.

References

[1] B. Zoheir, A. Beiranvand, and S. Kamh, “Shear-related gold ores in the Wadi Hodein Shear Belt, South Eastern Desert of Egypt: analysis of remote sensing, field and structural data,” Egypt, p. 36, April 30, 2021.

[2] M. Abd El-Wahed, B. Zoheir, A. B. Pour, and S. Kamh, "Shear-related gold ores in the Wadi Hodein Shear Belt, South Eastern Desert of Egypt: analysis of remote sensing, field and structural data," Minerals, vol. 11, no. 5, p. 474, 2021.

[3] H. Pian and M. Santosh, "Gold deposits of China: Resources, economics, environmental issues, and future perspectives," Geological Journal, vol. 55, no. 8, p. 5978-5989, 2020.

[4] I. EZZINE, F. ZARGOUNI, and M. GHANMI, "Lineamentary analysis of Landsat-TM and spot images from the Centro-Septentrional Atlas: mapping the SW extension of the Zaghouan scar", Revue Télédétection, Tunisia, p. 13, 2012.

[5] M. Mohammadpour, K. Alahveisi, and A. Bahroudi, "Automatic lineament extraction from ASTER images using the Hough transform, JabalBarez 1: 100000 sheet", Advanced Applied Geology, vol. 9, no 4, p. 374-391, 2020.

[6] H. Ahmadi, E. Pekkan, and G. Seyitoğlu, "Automatic lineaments detection using radar and optical data with an emphasis on geologic and tectonic implications: a case study of Kabul block, Southeast Afghanistan," Geocarto International, no just-accepted, pp. 1-71, 2023.

[7] Y. N. Akokponhoué, N. Yalo, H. B. Akokponhoué, M. Youan Ta, and G. Agbahoungba, "Contribution of Remote Sensing and Geophysics in the Mapping of Hydraulically Active Fractures in the Basement Zone in Central-West Benin," European Scientific Journal, Benin, p. 22, September 2019.

[8] S. Masurkar, "Lineament Mapping in the North-West Part of Gavilgarh Fault, Amravati District of Maharashtra Using SRTM DEM," International Journal of Research on Modernization of Engineering Science and Technology, India, July 7, 2023. Accessed: August 11, 2023. [Online]. Available at: www.irjmets.com

[9] R. Bouchra et al., "Lineament Extraction by Optical and Radar Images. The Case of Tan-Tan Province in Morocco," International Journal of Civil Engineering and Technology, Morocco, May 5, 2019. Accessed: August 9, 2023. [Online]. Available on: line on http://www.iaeme.com/ijciet/issues.asp?JType=IJCIET&VType=10&IType=5 ISSN Print : 0976- 6308

[10] M. Youan Ta, « Contribution of remote sensing and geographic information systems to the hydrogeological prospecting of the Precambrian basement of West Africa: case of the Bondoukou region (north-east of Côte d'Ivoire) ». COCODY UNIVERSITY, June 21, 2008.

[11] C. Adon Gnangui, S. Oularé, K. A. Kouamé, M. B. Saley, and K. F. Kouamé, "Automatic lineament extraction using optical and radar satellite images in the Precambrian basement environment (Haute Marahoué, Côte d'Ivoire," Cote d'Ivoire, p. 9, January 2019.

[12] P. Pandey and L. Sharma, "Image processing techniques applied to satellite data for extracting lineaments using PCI geomatica and their morph tectonic interpretation in the parts of northwestern Himalayan frontal thrust," Journal of the Indian Society of Remote Sensing, vol. 47, no. 5, pp. 809-820, 2019.

[13] E. Maryam, A. Ahmed, A. Abdellah, and F. Abdelouhed, "Mapping and analysis of structural lineaments using SRTM radar data and Landsat-8 OLI image: an example from the Telouet–Tighza area, Marrakech High Atlas, Morocco", Canadian Journal of Earth Sciences, 2023.

[14] P. M. MATAR, A. KARIFENE, and M. H. TAISSO, "Lineaments as a tool for decision-making in the optimal location of boreholes in the base zone: Case of the department of Abtouyour (republic of Chad)", 2023.

[15] P. M. MATAR, A. KARIFENE, and M. H. TAISSO, « Lineaments as a tool for decision-making in the optimal location of boreholes in the base zone: Case of the department of Abtouyour (republic of Chad) », 2023.

[16] A. Algouti, A. ALGOUTI, and A. FARAH, « Mapping and analysis of structural lineaments using SRTM radar data and Landsat 8-OLI images in Telouet-Tighza area, Marrakech High Atlas-Morocco. », 2022.

[17] B. Bessoles and R. Trompette, "GEOLOGY OF AFRICA, THE PAN-AFRICAN CHAIN "MOBILE ZONE OF CENTRAL AFRICA (SOUTHERN PART) AND MOBILE ZONE OF SUDANA"", 1980.

[18] M. G. Abdelsalam, J.-P. Liégeois, and R. J. Stern, "The saharan metacraton", Journal of African Earth Sciences, vol. 34, no. 3-4, p. 119-136, 2002.

[19] I. Kusnir and al., « Geology ,mineral resources and water resources of Chad ». 1995.

[20] J. G. Shellnutt, N. H. T. Pham, S. W. Denyszyn, M.-W. Yeh and T.-Y. Lee, « Timing of collisional and post-collisional Pan-African Orogeny silicic magmatism in south-central Chad », Precambrian Research, vol. 301, p. 113-123, 2017.

[21] M. Isseini, A. Hamit, and M. Abderamane, « The tectonic and geologic framework of the Mongo area, a segment of the Pan-African Guéra Massif in Central Chad: evidences from field observations and remote sensing », scientific review of Chad, vol. 1, no 3, p. 4-12, 2013.

[22] Z. Adiria and al., « Comparison of Landsat-8 satellite images, ASTER and Sentinel 1 Data of remote sensing de for automatic extraction of lineaments : case study of Sidi Flah-Bouskour inlier, Moroccan Anti », Advanced in Space Research, September 2017. [En ligne]. Disponible sur: http://dx.doi.org/10.1016/j.asr.2017.09.006

[23] M. R. Ranjbari, R. Vagheei, et H. Salehi, « Integration of Landsat-8 and Sentinel-1 dataset to extract geological lineaments in complex formations of Tepal mountain area, Shahrood, north Iran », Advances in Space Research, vol. 71, no 1, p. 936-945, 2023.

[24] P. Pandey et L. Sharma, « Image processing techniques applied to satellite data for extracting lineaments using PCI geomatica and their morphotectonic interpretation in the parts of northwestern Himalayan frontal thrust », Journal of the Indian Society of Remote Sensing, vol. 47, no 5, p. 809-820, 2019.

[25] A. Soliman and L. Han, « Effects of vertical accuracy of digital elevation model (DEM) data on automatic lineaments extraction from shaded DEM », Advances in space research, vol. 64, no 3, p. 603-622, 2019.

[26] T. Yao, O. Fouché-Grobla, M.-S. Oga, and V. Assoma, « Extraction of structural lineaments from satellites images and estimation of induced biases in the environment of metamorphosed Precambrian », Review of remote sensing Ivory Coast, p. 19, 2012.